# LASERS IN REMOTE SENSING FOR TERRESTRIAL AND HYDROGRAPHIC APPLICATIONS

Walter G. Egan

Natural Sciences Department, York College/
City University of New York, Jamaica, NY 11451

ABSTRACT

The application of lasers in remote sensing conventionally involves a monostatic approach, with the laser and sensor nearly exactly coaligned. This arises from the practical consideration where the remote sensing platform holds the both the laser and sensor in close proximity. A major problem in such a system is the calibration for retroreflection, which may amount to up to a factor of 10 above that for a diffuse ground calibration target. The amount of retroreflection peaking depends not only upon the calibration target, but also on the target to be sensed, as well as the polarization properties of the illuminating laser.

The optical properties of various natural and man made calibration target materials will be discussed in the wavelength range from the ultraviolet to the near infrared. An attempt will be made to guide the user in the design of polarizing remote sensing systems to enhance contrast.

Key Words: lasers, polarization, remote sensing, retroreflection, calibration, coherence, standards, farm crops, agriculture

## 1. INTRODUCTION

The use of lasers in remote sensing for terrestrial and hydrographic applications implies active systems whereby either a pulsed or continuous wave laser source is used to illuminate a scene. The illuminating may be accomplished full field or by scanning, and the returned scattered energy continuously sensed or gated.

A significant factor in the return of scattered laser (as well as low coherence) radiation occurs as retroreflection by a surface. Retroreflection by a surface occurs when the source and sensor are coaligned as frequently occurs in laser sensing systems. Retroreflection by a surface is defined as a non-linear brightness increase as the source-surface-observer angle is decreased to exactly zero degrees.

For instance, in Fig. 1, the reflectance of a "diffuse surface" is shown as a function of viewing angle. The diffuse surface is a magnesium carbonate block (freshly scraped), and the usual cosine reflectance appears, except for a sharp non-linear peaking at exactly zero degrees. The peaking in the figure is shown for incandescent illumination, but the peaking also occurs for



Part of the SPIE Conference on Advances in Laser Remote Sensing for Terrestrial and Hydrographic Applications
Orlando, Florida • April 1998 SPIE Vol. 3382 • 0277-786X/98/$10.00

unpolarized laser illumination (Fig, 2), in a different way. The peaking amounts to about 130% of the diffuse reflection for this sample. What this means is that the diffuse surface is not diffuse in retroreflectance, and the use of diffuse surface as a reflectance standard is not valid in retroreflectance. (The deviation from diffuseness may be a great as an order of magnitude, as described in the following). Thus, in laser remote sensing, considerable care must be exercised in calibration procedures. The retroreflectance peaking generally depends upon the type of surface and the source collimation, and oddly enough it is independent of the tilt of the surface to the incident laser beam (Figs. 3 and 4).

## 2.LASER REMOTE SENSING SYSTEMS CONSIDERATIONS

There are two general classifications of laser remote sensing systems: 1) civilian, and 2) military, with the subsidiary classes : 1) daytime, and 2) nighttime. All weather systems, while more complicated, form a further class. Real time systems form another class of laser remote sensing systems, with detectability becoming very significant for military applications. In the following discussion, only a few aspects will be considered.

By far laser optical systems are based on photometry - brightness variations in scenes as a function of targets and illuminating and viewing geometry. Polarization is a weak cousin to photometry. Although optical polarization is an important factor in astronomy and astrophysics, its significance in laser optical remote sensing has lagged. Conventional lasers are generally unpolarized, because of the simplicity of constructing a laser with random polarization. The requirement of a Brewster angle mirror adds a complication which can also reduce laser output.

Why should we be concerned with polarization in laser remote sensing?

To answer this question, we must delve into the polarimetric properties of laser targets and the relevance of polarization.

First, we must set the stage for polarization: the kinds of polarization, detectability, spatial and temporal coherence.

## 3.TYPES OF POLARIZATION

We are all familiar with plane polarization, from sunglasses designed to remove sun glare from secular reflection from water surfaces, to the use of polarizing (at 45 degrees) glasses for stereo viewing of projected polarized images. In photography, polarizing filters are used to enhance sky contrast, because the sky is generally highly polarized. Even so, single lens reflex cameras have polarizing optics in the exposure mechanism which necessitates the use of a circular polarization filter to eliminate undesirable effects.

"Natural" light is generally never completely unpolarized, with plane polarization produced by reflection from surfaces. Plane polarization is a directional vector property of radiation whereby the electric field is in a specific direction (and the magnetic field perpendicular). To relate to radio, a dipole antenna produces (or senses) polarized radiation directed along the length of the dipole. TV antennas are generally horizontal and thus are optimized to detect horizontally polarized radiation. Thus plane polarized radiation has a preferred direction, with the direction produced by the source. Circular polarized radiation is produced by the combination of mutually plane polarized radiation with a 90 degree temporal phase shift between the spatial components. Elliptical polarization is a combination of circular and plane polarization. These aspects of polarization are characterized by the Stokes Vector (I,Q,U,V)[5].

## 4.REPRESENTATION OF POLARIZATION

There are two computational techniques for treating polarization: 1) the Jones calculus and 2) the Mueller calculus. Whereas the Jones calculus is simpler and describes the absolute phase of light, it will not treat problems involving depolarization and light scattering; Mueller calculus will and is preferable experimentally where depolarization and scattering are measured. In the Mueller calculus, the four components of the Stokes vector describe the elliptical polarization of light and the degree of polarization. The Stokes vector describes the angular coherence of the radiation, the amplitudes, phase and statistics of the electromagnetic waves. Polarizing properties of surface scattering are described at each wavelength by the four element Stokes vector.

## 5.SYSTEM CALIBRATION

Because of retroreflectance, one cannot arbitrarily assume the reflectance of a ground calibration target; the theory of laser retroreflectance is incomplete and the retroreflectance must be measured a ground level not only for the calibration target but for the surface or structure being sensed. Since the scale of the structure being sensed affects the retro effect, the size of the image remotely sensed must be simulated a ground level.

One approach that was used in lunar surface polarimetric simulation for the moon landing program, was the measurement of simulated lunar surfaces with a large scale photometer/polarimeter. Thus the scale of rocks as well as powders could be represented accurately experimentally for photometry and polarization for comparison to astronomical data for the lunar surface. A similar approach is applicable for remote sensing system polarization calibration.

## 6.APPLICATIONS

There are a number of theories to account for retroreflection. One theory involves large scale shadowing, This effect is apparent when one views the foliage covered ground from an aircraft. A halo appears around the shadow of the aircraft with a brightening at the center. At exactly in the retro direction, there are no shadows and a brightening appears.

A second theory involves weak field localization, an electromagnetic field scattering effect, whereby two scattered rays from a surface interfere to cause an amplitude increase up to a factor of two. A third theory related to the second theory also involves coherent interference from surface retroreflection to cause an amplitude increase by a factor of two or more. Under certain conditions when a structure or surface has a linement parallel to the electric field direction of a laser, peaking may be up to orders of magnitude (as with horizontal electric or telephone lines).

Examples of high resolution retroreflectance,using the system in Fig 5, are shown in Figs. 6-9; various surfaces exhibit an increase up to a factor of two or more. Figure 6 shows retroreflection for a soil (limonite powder) in four polarization orientations of source and sensor (these correspond to microwave orientations HH, HV, VV, and VH, where H corresponds to parallel and V corresponds to vertical). It is seen that a flowere of sulfur surface shows negligible retroreflectance peaking, but a limonite powder does. Note that there is no retro in cross polarization.

If we go to higher angular resolution (0.057 degree as shown in Figs. 9a, 9b, 9c), an additional reproducible retroreflection structure appears, caused by interference in radiation scattered from various facets on the surface. The C position indicates the exact retrodirection determined by autocollimation. Here, depending upon the reference direction, retro may be more or less than a factor of two.

An application of retroreflection is shown in Fig. 10 for ice/water clouds. Here depolarization is shown for LIDAR as a function of time from a 2 km thick cirrostratus cloud; ice crystals because of their crystalline shapes, depolarize more strongly than spherical water droplets, and depolarization is greater with increase in altitude (decrease in temperature).

Table 1 lists laser retroreflectance ( 0.6328 um) for various types of surfaces as a guiode as to what to expect. Table 2 lists the 3 degree albedo on various foliage and farm crops as well as specularity in 0.633 $\mu$m low spectral coherence radiation. The 3 degree albedo is an index of retroreflection without taking into account the retro peaking; the foliage consists of random scattering facets, and the specularity is an indication of the specular reflectance of the same facets. Thus, even with low coherence illumination we can get an uncalibrated indication to characterize the polarization scattering properties of farm crops and foliage. It is to be noted that there is an inverse relationship between Geometric Albedo and the Approximate Average Percent Polarization; this same relationship has been noted in lunar surface simulation. Apparently dark surfaces involve internal scattering, whereas bright surfaces have enhanced external scattering and appear whiter.

The results of such a characterization using Space Shuttle polarization imagery at a wavelength of 0.633 um are shown is Figs. 11 and 12. It is seen that hydrological and terrestrial features are chacterized; even though a laser was not used, the relationship to polarized low coherence (solar) radiation is evident as inferred from the relationships shown in Figs. 1 and 2.

Another application of polarization is the laser detection of personnel in a jungle environment. The clothing of a person (or skin) is pretty much diffuse, whereas the leaves of plants are highly polarized in the 0.4 to 0.5 $\mu$m spectral region. Thus the reduction in polarization by the target in plane polarized (or circularly polarized) can enhance contrast by a factor of two or more.

Laser detection of aircraft against the polarized sky background (or polarized foliage covered ground) can be enhance by suitably orienting the laser source polarization relative to the polarization sense of the detection system.

## 7. SUMMARY

From the foregoing discussion, it is clearly evident that calibration is necessary to establish quantitative values to laser retroreflectance measurements. A factor of two or more in retroreflectance calibration may seem unimportant, but the significance is of utmost importance when quantitative observations are made in remote sensing. Small differences in calibration, especially in polarization, can render a program unsuccessful. Since polarization is highly accurate photometry, and as such requires accurate calibration techniques to become and remain useful in the many possible future applications.

## 8. REFERENCES


1. Walter G. Egan and Theodore W. Hilgeman, Optical Properties of Inhomogeneous Materials, Academic Press 1979, 235 pp.
2. Walter G. Egan, Laser retroreflectance consistent with a polarized single-scatter weak electromagnetic-field localization-interference phenomenon, Appl. Opt. 33, Jan 1994. pp535-543.
3. Walter G. Egan, Editor, Polarization and Remote Sensing, Vol. 1747, Proceedings of International Society for Optical Engineering, 22-23 July 1882, San Diego, CA.
4. W. G. Egan, S. Israel, W. R. Johnson, and V. S. Whitehead High resolution Space Shuttle photometry for farm crop classification, Appl. Opt. 31, 1992, pp.1542-1548.
5. Walter G. Egan,Photometry and Polarization in Remote Sensing, Elsevier, New York, 1985, 503 pp.



Correspondence: Email: EGAN@YCVAX.YORK.CUNY.EDU;
Telephone/FAX (718) 441-6210

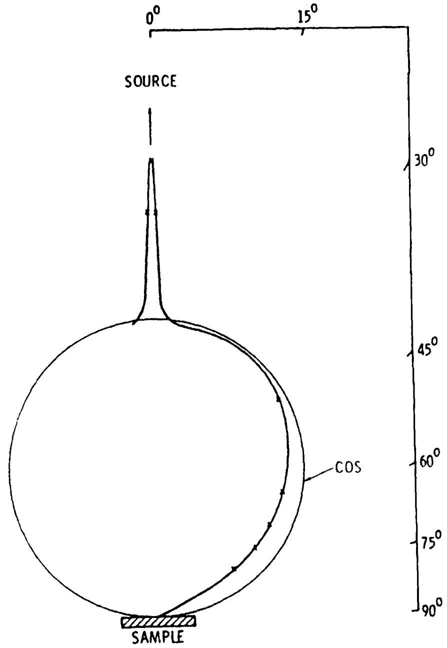


Fig. 1 Reflectance properties of $BaSO_4$ coating at $\lambda = 0.6$ $\mu m$ with low-coherence illumination. 1

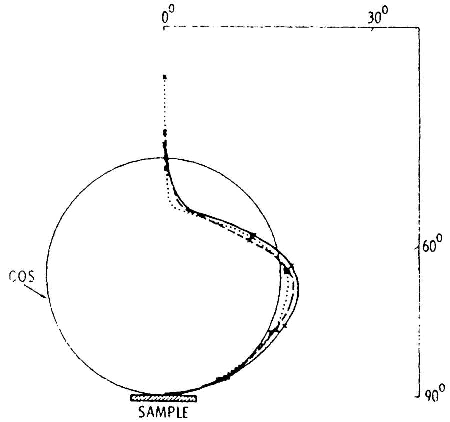


Fig. 2 Reflectance properties of $BaSO_4$ (---), $MgCO_3$ (——), and sulfur (· · ·) with high-coherence illumination (0.6328-$\mu m$ He–Ne laser). 1

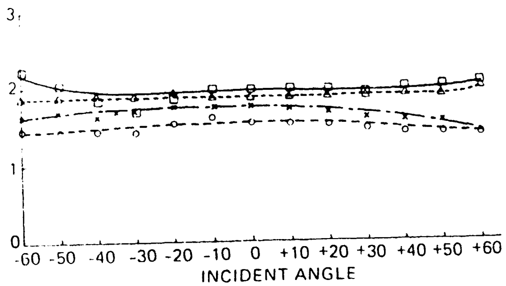


Retroreflectance effect at varying incident angles for $BaSO_4$ (×), $MgCO_3$ (○), white Nextel paint (△), and colloidal sulfur (□) for $\lambda = 0.6328$-$\mu m$ He–Ne laser illumination with 1° source collimation and sensor acceptance angles. 1

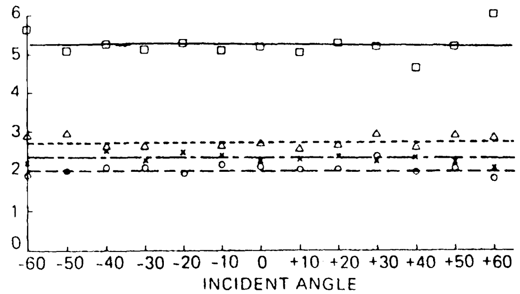


Fig. 4 Retroreflectance effect at varying incident angles for $BaSO_4$ (×), $MgCO_3$ (○), white Nextel paint (△), and colloidal sulfur (□) for $\lambda = 0.6328$-$\mu m$ He–Ne laser illumination with better than 1° source collimation and sensor acceptance angles. 1

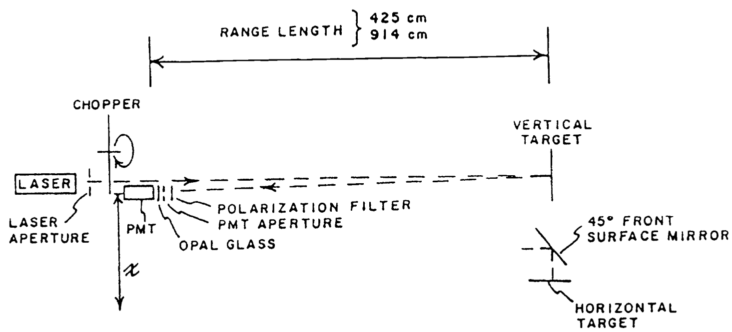


Fig. 5 Laser range I: Layout showing laser and adjacent photomultiplier, chopper, baffles, and polarization filter. Targets may be placed vertically, or for powders, horizontally with the use of the 45° mirror. [2]

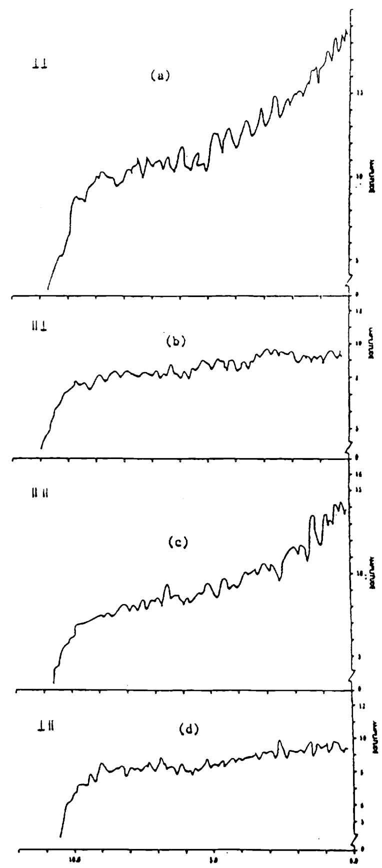


Fig. 6 Retroreflection amplitudes as a function of the included angle of limonite powder <1 μm at 0.6328 μm laser wavelength for four laser-analyzer orientations on 425-cm range. Optical angular resolution = 0.14 degrees. [2]

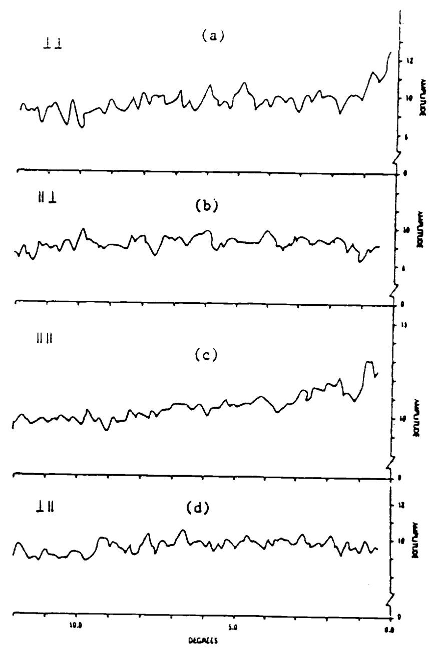


Fig. 7 Retroreflection amplitudes as a function of the included angle layer of deposited flowers of sulfur at 0.6328 μm laser wavelength for four laser-analyzer orientations on 425-cm range. Optical angular resolution = 0.14 degrees. [2]

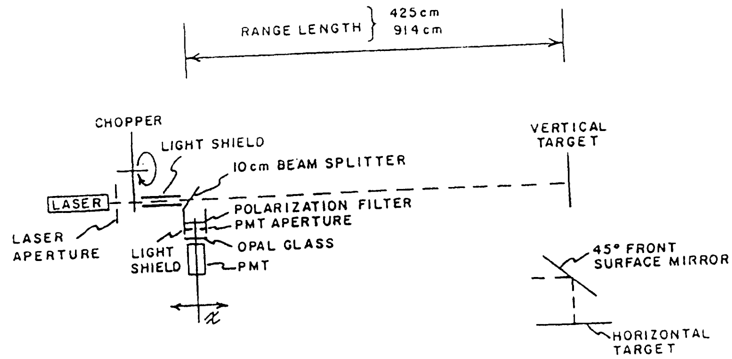


Fig. 8 Laser range II: Layout showing laser and perpendicular photomultiplier viewing the 10-cm-diameter beamsplitter. Appropriate baffles are provided. Targets may be placed vertically, or for powders, horizontally with the use of the 45° mirror. [2]

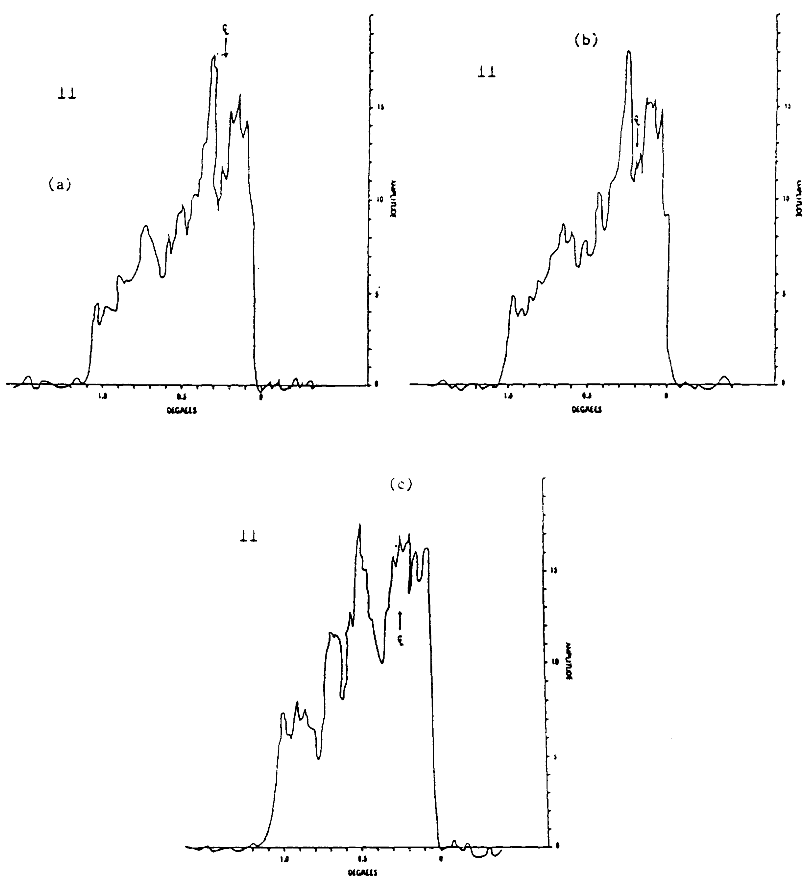


Fig.9 Retroreflection amplitudes for perpendicular-perpendicular orientations on sulfur; (a) and (b) are repeat runs, and (c) is surface tilted at 10 degrees relative to (a) and (b). Optical angular resolution is 0.057 degrees. [2]

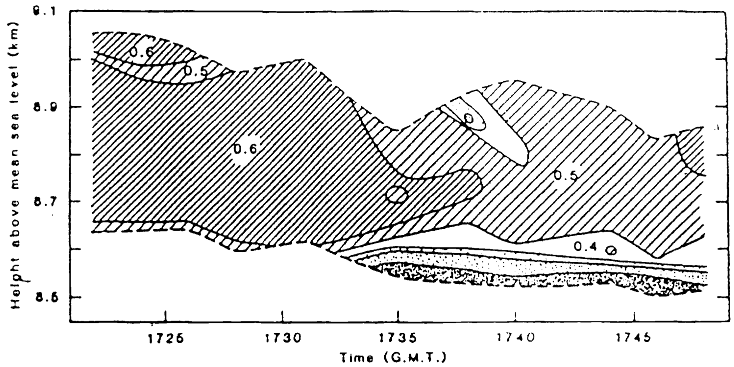


Fig. 10 Height versus time display of linear depolarization ratios generated from vertically pointing lidar measurements during the initial appearance of highly supercooled liquid water at the bottom of a 2-km-thick cirrostratus cloud on 17 October 1983. A gradual water-to-ice cloud transformation is shown by the decreasing stippling just above the cloud base. The cloud boundaries (dashed lines) derived from the δ value analysis often do not correspond to the actual cloud boundaries, particularly in the presence of significant optical attenuation. 3

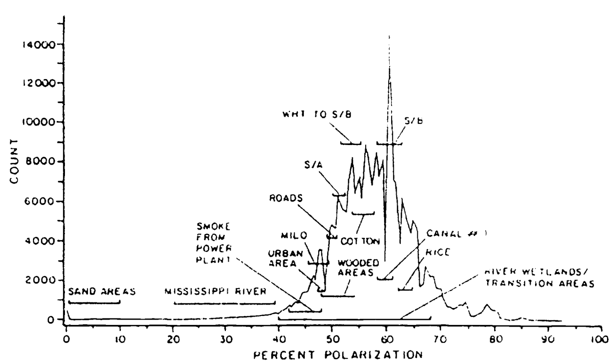


Fig. 11 Breakout of the red percent polarization band identifying the peaks with corresponding ground features.

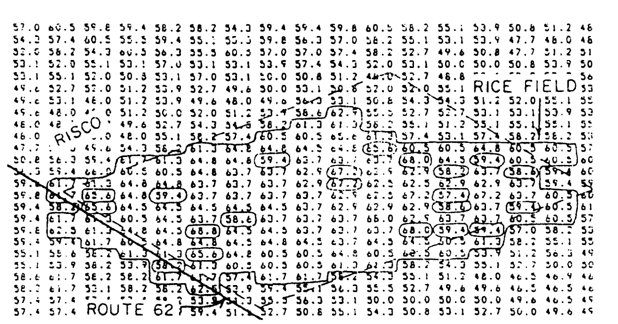


Fig. 12 Digital output of the red band percent polarization showing a 122.6-acre (0.506-km$^2$) rice field. Encircled values within the field lie outside the recognition range of 60.5%–64.8% polarization. 4

TABLE 1
RETROFLECTION SUMMARY

| Sample | Retro ⊥ ⊥ | Retro ∥ ∥ | Cross Pol Retro ∥ ⊥ | Cross Pol Retro ⊥ ∥ | Resolution |
|---|---|---|---|---|---|
| Sulfur | 2.8 | 3.3 | 2.8 | 3.5 | High |
| Sulfur | 1.4 | 1.5 | -- | -- | Low |
| Glass Beads (25), 1mm dia | 1.5 | 1.5 | -- | -- | Low |
| Glass Beads (1), 1 mm dia | 1.7 | 1.8 | -- | -- | Low |
| Plexiglass rods, 1.8 mm d | 70 | 90 | -- | -- | Low |
| Plexiglass rods, 45 deg | 95 | 67 | 18R | 19R | Low |
| Copper wool | 2.7 | 2.2 | 2.0 | 1.6 | Low |
| Sugar | 1.4 | 1.6 | 1.3S | 1.2S | High |
| Halon | 1.1 | 1.1 | -- | -- | Low |
| Halon | 3.0 | 2.3 | 1.5R | 1.7R | High |
| $MgCO_3$ | 1.5 | 1.5 | -- | -- | Low |
| $MgCO_3$ | 3.3 | 2.5 | 1.3R | 1.5R | High |
| White Nextel | 2 | 2 | -- | -- | High |
| Red Nextel | 1.6 | 1.8 | -- | -- | Low |
| $BaSO_4$ | 1.5 | 1.5 | 1.2S | 1.2S | Low |
| Anatase Powder | 1.8 | 1.4 | 1.1 | -- | Low |
| Anatase Paint | 1.8 | 2.0 | -- | -- | Low |
| Limonite, compact <1μm | 2.0 | 1.8 | -- | -- | Low |
| Limonite, powder <<1μm | 2.0 | 1.8 | -- | -- | Low |
| Limonite, powder <1μm | 2.0 | 2.0 | 1.1S | 1.1S | Low |
| Aluminum, powder <37μm | 1.3 | 1.3 | -- | -- | High |
| Aluminum, powder 88-150μm | 1.3 | 1.2 | -- | -- | Low |
| Copper shot, oxidized | -- | -- | -- | -- | Low |
| Wire grid polarizer | 1.8 | 1.8 | -- | -- | High |
| Al powder, spher. udx-65 | 1.5 | 1.3 | -- | -- | High |
| Xerox white paper | 1.4 | 1.4 | -- | -- | Low |
| Limonite paint | 2.0 | 1.8 | -- | -- | Low |
| Bytownite, 0° tilt | 140 | 105 | -- | -- | Low |
| Bytownite, 1° tilt | 17 | 6.3 | -- | -- | Low |

TABLE 2

SPECTROPOLARIMETRIC CHARACTERIZATION OF FARM CROPS AND SOILS
(0.633 $\mu$m wavelength)

| Material | Geometric Albedo | Approx.Avg.%Polarization |
|---|---|---|
| Alflfa Leaves | .075 | 13.3 |
| Potato Leaves | .053 | 75.3 |
| Corn Leaves | .070 | 40.1 |
| Corn Tassels | .202 | 10.6 |
| Wet Farm Soil(20.6%$H_2O$) | .097 | 26.3 |
| Dry Farm Soil | .258 | 9.1 |
| Rye Stalks | .396 | 7.3 |
| Wheat Stalks | .471 | 7.7 |
| Rye Heads | .223 | 9.3 |
| Wheat Heads | .276 | 8.7 |
| Fresh Red Pine Needles | .055 | 36.2 |
| Dry Red Pine Needles | .148 | 20.0 |
| Red Pine Bark | .104 | 31.0 |
| Black Oak Leaves | .0175 | 74.6 |
| Sugar Maple Leaves | .034 | 43.0 |
| Fresh Peach Leaves | .019 | 27.2 |